

Design and biofabrication of dermal regeneration scaffolds: role of oligomeric collagen fibril density and architecture

David O Sohutskey^{‡,1,2} , Kevin P Buno^{‡,1}, Sunil S Tholpady^{3,4}, Samantha J Nier¹ & Sherry L Voytik-Harbin^{*,1,5}

¹Weldon School of Biomedical Engineering, Purdue University, West Lafayette, IN 47907, USA

²Medical Scientist Training Program, Indiana University School of Medicine, Indianapolis, IN 46202, USA

³Division of Plastic Surgery, Department of Surgery, Indiana University, IN 46202, USA

⁴Division of Plastic Surgery, Richard L. Roudebush Veterans Affairs Medical Center, Indianapolis, IN 46202, USA

⁵Department of Basic Medical Sciences, Purdue University, West Lafayette, IN 47907, USA

*Author for correspondence: harbins@purdue.edu

‡ Authors contributed equally

Aim: To evaluate dermal regeneration scaffolds custom-fabricated from fibril-forming oligomeric collagen where the total content and spatial gradient of collagen fibrils was specified. **Materials & methods:** Microstructural and mechanical features were verified by electron microscopy and tensile testing. The ability of dermal scaffolds to induce regeneration of rat full-thickness skin wounds was determined and compared with no fill control, autograft skin and a commercial collagen dressing. **Results:** Increasing fibril content of oligomer scaffolds inhibited wound contraction and decreased myofibroblast marker expression. Cellular and vascular infiltration of scaffolds over the 14-day period varied with the graded density and orientation of fibrils. **Conclusion:** Fibril content, spatial gradient and orientation are important collagen scaffold design considerations for promoting vascularization and dermal regeneration while reducing wound contraction.

First draft submitted: 8 July 2019; Accepted for publication: 2 March 2020; Published online: 31 March 2020

Keywords: custom fabrication • mechanobiology • oligomeric collagen • regeneration • skin and wound care

Difficult-to-heal and chronic wounds of the skin are among the most common and costly medical problems experienced. A variety of mechanisms can lead to such wounds, such as trauma, burns, oncologic resection or systemic disease [1], with the scope and magnitude of therapy varying significantly with individual age, etiology and severity. For nonhealing and large wounds, autologous split-thickness skin grafts can be a reasonable option despite limitations in their availability and capacity to fully recapitulate dermal function which leads to frequent scarring and contracture [2]. These tissue grafts also suffer from low take rates, especially in cases of chronic wounds due to systemic disease [3]. As an alternative, several dermal substitutes have been developed and are commercially available. Of these, the most prevalent are decellularized scaffolds derived from xenogeneic or allogeneic tissues (e.g., placenta and dermis) and bioengineered resorbable collagen sponges fashioned from fibrillar collagen microparticulate in the presence or absence of glycosaminoglycans (GAGs). These dermal replacements are also generally slow to cellularize and vascularize, requiring host-cell deposition of collagen as the scaffold actively degrades (resorbs) via an inflammatory mediated process [4]. Additionally, cellularization is often accompanied by myofibroblasts, known contributors to wound contraction and contracture [2,5,6]. Collectively, it is for the above stated reasons that a need exists for new therapeutic approaches designed to accelerate wound closure and improve dermal regeneration to reduce morbidity and mortality associated with difficult-to-heal wounds.

Normal healing of acute skin wounds, where both the epidermal and dermal layers are breached, is a well-orchestrated 'repair' process. This process involves four overlapping phases including hemostasis, inflammation, granulation and remodeling/maturation, with the length of these phases varying based on wound etiology and severity [7]. Large surface area and chronic (remain unhealed for >12 weeks) wounds, on the other hand, fail to

proceed through these phases in an orderly fashion. Although these wounds vary significantly, common features include prolonged or dysregulated inflammation and excessive destruction (proteolytic degradation) or contraction of the newly deposited collagen matrix [8]. The lack of sufficient and persistent dermal collagen within the wound space not only prevents the wound from moving forward in the healing process but also leads to the influx of more inflammatory cells thus amplifying the inflammation cycle [9]. This situation is further exacerbated in elderly patients or certain pathological conditions (e.g., diabetes), where wound healing is characterized by delayed and reduced collagen deposition, delayed vascularization and increased senescence of fibroblasts and relevant stem/progenitor cell populations [7].

The dermal layer of skin is primarily comprised of a fibrillar type I collagen extracellular matrix (ECM), which is responsible for imparting both structural and mechanical integrity. For this reason, substantial emphasis has been directed toward development of dermal substitutes that recapitulate various compositional and physical features of the native dermal ECM, such as the collagen microstructure and the complex macromolecular composition including growth factors [10]. Additionally, there has been increasing interest in defining the multiscale physical forces between cells and the surrounding collagen scaffold and their role in modulating fundamental cell behavior as well as tissue generation [11,12]. This perspective of mechanobiology highlights the fact that cells probe, attach and tug on (remodel) the fibrillar scaffold via specific cell surface receptors known as integrins. The mechanical forces experienced at these linkages in turn result in activation of downstream mechanochemical signaling pathways ultimately regulating cell phenotype and function. In the case of wounds, this hierarchical mechanochemical signaling imparted by the dermis is disrupted and the physical context of the surrounding tissue scaffold and constituent cells dramatically altered [11]. The loss of mechanical stability requires host cells to produce, deposit and remodel their own new ECM, delaying healing and leading to complications such as fluid loss, infection and scarring. Here, we converge principles and practices of mechanobiology and collagen polymer-based material customization with the goal of prioritizing design criteria for the scalable fabrication of mechano-instructive fibrillar collagen scaffolds for dermal regeneration.

Our bioinspired design strategy involves type I oligomeric collagen, a highly-purified, fibril-forming collagen that, unlike monomeric formulations (e.g., atelocollagen and telocollagen), retains natural intermolecular crosslinks [13]. Conventional monomeric collagens that are acid-solubilized and purified from tissues represent single triple-helical molecules (telocollagen: full length tropocollagen molecule; atelocollagen: truncated tropocollagen molecule) consisting of three polypeptide chains (typically two $\alpha 1$ chains and a single $\alpha 2$ chain). Oligomeric collagen, in contrast, represents acid-soluble aggregates of collagen molecules (e.g., trimers of tropocollagen molecules) that are covalently bonded by a crosslink chemistry produced by the lysyl oxidase family of enzymes during *in vivo* collagen assembly [13,14]. Differences between atelocollagen, telocollagen and oligomeric collagen have been documented, including their molecular composition, average molecular weight and, most importantly, *in situ* fibril-forming capacity upon neutralization (i.e., their inherent capacity to undergo self-assembly to form fibrillar matrices) [13–15]. Compared with monomeric collagen, oligomers display more rapid fibril formation (~ 60 s at body temperature), yielding matrices (scaffolds) with increased fibril–fibril connectivity. The increased connectivity between fibrils, together with the presence of natural intermolecular crosslinks, contributes to improved stability (shape retention; resistance to proteolytic degradation) and mechanical properties of formed fibrillar scaffolds [13,15,16]. Further, *in vitro* studies show that differences between oligomer and monomer scaffolds can be sensed by cells, with the increased resistance to cellular traction forces provided by oligomer scaffolds modulating fundamental cell behavior, including proliferation, migration, differentiation and tissue morphogenesis [13,14,17,18]. Since collagen oligomers overcome a number of apparent limitations inherent to monomeric formulations, our group continues to evaluate their utility as a platform natural polymer for a variety of tissue engineering and regenerative medicine applications (see [19] for a recent review).

When formed at relatively low fibril content (≤ 5 mg/ml), oligomer scaffolds can be further processed via confined compression to controllably reduce the interstitial fluid content and increase the overall content of collagen fibrils (weight percent of fibrillar collagen). This scalable biofabrication technique, which represents a modified version of collagen gel compression methods described by Brown and coworkers [20], has been applied for customization of scaffolds varying in geometry and overall fibril content as well as creation of scaffolds with continuous gradients of varying fibril density (porosity) and/or fibril orientation [16,21]. In this way, anisotropic properties displayed by the fibrillar collagen component of tissues can be better approximated and the contributions of cell-collagen mechanochemical signaling during tissue remodeling and regeneration elucidated.

In the present study, we hypothesized that the total content and spatial gradient of collagen fibrils, as controlled by confined compression, are important determinants of oligomer scaffold mechanics and the *in vivo* tissue response following application to rat full-thickness excisional wounds. More specifically, based on previous work, we anticipated that increasing the total fibrillar collagen content would increase the mechanical modulus and strength of scaffolds and reduce wound contraction, while providing a barrier to cellular infiltration. As such, we hypothesized that fabrication of scaffolds with a spatial gradient in collagen fibrils, progressing upward from low-to-high collagen-fibril content (i.e., high to low porosity) would facilitate cellularization and vascularization while maintaining the necessary macro-scale mechanical properties. First, cryogenic scanning electron microscopy (cryo-SEM) and tensile mechanical testing were used to define the microstructure and bulk tensile properties of bioengineered oligomer scaffolds compared with normal rat dermis and HeliCote. HeliCote was selected for comparison since it represents a bioengineered collagen wound dressing fabricated from fibrillar collagen microparticulate and is noncrosslinked [22]. Next, oligomer scaffolds, along with the commercial dressing, autograft skin and no fill controls, were evaluated in an established rat full-thickness excisional skin model, where gross appearance and wound contraction were measured over a 14-day period. Harvested tissues were processed and analyzed histologically for general tissue response, as well as specific markers of myofibroblast activation and tissue vascularization.

Materials & methods

Controlled confined compression device for oligomer dermal scaffold fabrication

Oligomer dermal scaffolds were fabricated with a custom-designed confined compression device (Figure 1). The device consisted of a compression head that was designed in SolidWorks (MA, USA) and 3D-printed using a Stratasys 3D Printer (Stratasys, MN, USA) for use with a standard 24-well culture plate. The compression head was adapted with small cylinders (1.5-cm diameter) of porous polyethylene foam (0.25" thick, 50 μm pores; Scientific Commodities Inc., AZ, USA). Indentations drilled into the center of each foam cylinder allowed press-fitting onto the compression head. The compression head was sterilized with gas plasma for 30 min, after which foam ends were rinsed with sterile phosphate-buffered saline (PBS) to remove any residuals.

Oligomer dermal scaffolds & commercial collagen dressing

Oligomer dermal scaffolds representing various total content and spatial gradients of collagen fibrils were fabricated from type I oligomeric collagen derived from the dermis of market-weight pigs as described previously [13]. Before use, lyophilized collagen was dissolved in 0.01 N hydrochloric acid and concentration determined by a Sirius red assay. To induce polymerization (self-assembly) of collagen-fibril scaffolds, acidic solutions of oligomer were neutralized to physiologic pH and ionic strength with a proprietary neutralization reagent and warmed to 37°C. All oligomeric collagen formulations were standardized based on molecular composition and polymerization capacity in accordance with American Society for Testing and Materials, is (ASTM) International standard F3089-14 [23]. Here, polymerization capacity is defined by the shear storage modulus (G' , Pa) of a polymerized scaffold as a function of oligomer concentration of the polymerization reaction [13]. The resultant polymerization capacity curves for an oligomeric collagen formulation must be consistent with our historic database [13] to be deemed acceptable.

To fabricate oligomer dermal scaffolds, neutralized oligomer solutions (4.0 mg/ml) were pipetted into 24-well plates at specific volumes (230, 1150 and 2300 μl) and polymerized at 37°C. Following polymerization, wells containing 230- μl oligomer were not further processed, yielding 4 mg/cm³ scaffolds (Oligomer-4) with a diameter of 15.6 mm and thickness of 1.2 mm. This thickness was chosen to approximate the thickness of rat dermis [24]. Wells containing 1150 and 2300 μl oligomer were subjected to controlled confined compression [16,21] to a thickness of 1.2 mm, yielding 20 mg/cm³ (Oligomer-20) and 40 mg/cm³ (Oligomer-40) scaffolds, respectively. Confined compression at a strain rate of 0.1/s was conducted with the compression head adapted to a universal mechanical testing machine (TestResources, MN, USA). All oligomer dermal scaffolds were stored in sterile PBS prior to surgical implantation.

HeliCote, a commercial collagen wound dressing, was obtained from Integra Miltex (PA, USA). HeliCote is manufactured via a proprietary methodology that involves lyophilization of a slurry of comminuted bovine tendon, yielding a freeze-dried collagen sponge.

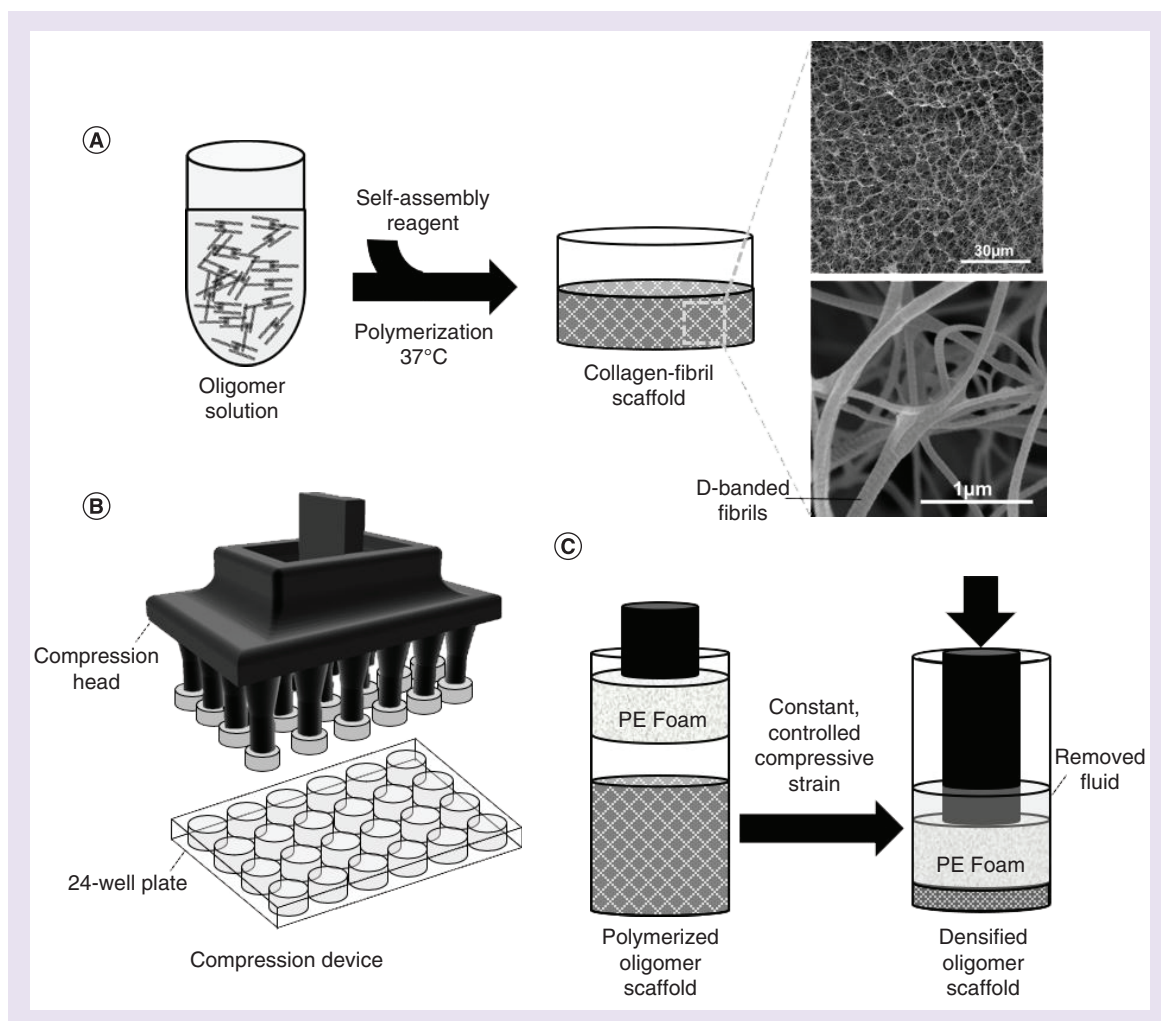


Figure 1. Process diagrams for preparation of oligomer dermal scaffolds. (A) Acid-soluble oligomer solution (4 mg/ml) was neutralized and polymerized at 37°C, yielding a low-density oligomer matrix. (B) Schematic of confined compression device, featuring a compression head with PE foam platens. (C) Application of different levels of strain in a confined compression format to low-density matrices yields densified scaffolds that vary in total content and spatial gradient of collagen fibrils. PE: Porous polyethylene.

Ultra & microstructure analysis

Ultra and microstructure analysis of oligomer dermal scaffolds, commercial collagen dressing and normal rat dermis was performed via cryo-SEM using an FEI NOVA nanoSEM 200 (FEI, OR, USA) varying between an Everhart-Thornley (<10,000× magnification) or immersion lens (>10,000× magnification) detector [16]. Samples were flash-frozen by submersion into critical point liquid nitrogen, transferred to a CT1000 cold-stage attachment (Oxford Instruments North America, Inc., MA, USA) and sublimated under vacuum. Samples were subsequently sputter coated with platinum and imaged. Images (15,000× magnification) were analyzed using FIJI/ImageJ (NIH, MD, USA) and the Directionality tool used to create histograms of fibril orientation. To analyze porosity, the DiameterJ plugin was used to binarize the images using a statistical region-merging algorithm [25,26]. The Analyze Particles tool was used to measure pore diameters.

Rat full-thickness excisional skin model

All animal studies were conducted according to protocols approved by the Purdue University Institutional Animal Care and Use Committee. Male Sprague-Dawley rats, weighing 200–250 g (7–9 weeks of age; Charles River Laboratories, MA, USA), were anesthetized using isoflurane gas. A sterile punch (15 mm diameter) was used to

create a total of two full-thickness skin wounds, including the panniculus carnosus muscle, positioned on either side of the sagittal plane of the rat dorsum. Wounds were randomly assigned to experimental treatment and control groups, with experimental treatment groups consisting of Oligomer-4, Oligomer-20, Oligomer-40, and commercial collagen dressing ($n = 4-10$). Oligomer-20 and Oligomer-40 samples, which exhibited sidedness owing to the graded microstructure, were positioned with their more porous (less dense), isotropic region on the bottom of the wound bed. For a subset of animals, the excised full-thickness skin was applied to the opposite wound, serving as an autograft (positive control). Wounds left as unfilled (no fill) served as negative controls. Materials with sufficient handling and suturability, specifically Oligomer-20, Oligomer-40 and autograft, were sutured into place with nonabsorbable 5-0 silk sutures (Perma-Hand Silk, Ethicon, NJ, USA). All wounds were covered with an occlusive petrolatum gauze to prevent moisture loss (XeroformTM, Covidien, Dublin, Ireland), a nonadherent pad (McKesson, CA, USA) and an adhesive film dressing (Tegaderm, 3 M, MN, USA). For additional support, the rats were wrapped with self-adherent cohesive bandages (VetRap, 3 M, MN, USA) and secured with a nonstretch porous tape (ZONAS, Johnson & Johnson, Inc., TX, USA). Investigators were not blinded to treatment groups due to the apparent visual and handling differences between implant materials.

Dressing changes were performed at 7 days or as needed. Photographs of wound areas were taken with a ruler in the field of view at 0, 7 and 14 days. At 7- and 14-day study end points, animals were euthanized and wound areas and associated implants were excised *in toto* and processed for histopathological analysis. Absolute wound areas were quantified using a MATLAB (The Mathworks, MA, USA) script and normalized to original wound areas. Autografts that did not successfully take after 7 days, as determined by visual color changes indicating extensive tissue necrosis, were not included in the analysis.

Histopathological analysis

Excised tissue was fixed in 4% paraformaldehyde for at least 24 h and then transferred to PBS. Bisected samples were embedded in paraffin and sectioned (4- μ m thickness). Sections were stained with hematoxylin and eosin and Masson's Trichrome for general histopathological analysis. Additional paraffin sections were stained with primary antibodies for alpha-smooth muscle actin (α -SMA; ab5694, Abcam, Cambridge, UK; 1:500 dilution) and CD31 (AF3628SP, R&D Systems, MN, USA; 1:50 dilution). After incubation with a secondary antibody (GoRb ImmPRESS HRP, Vector Laboratories, CA, USA) according to manufacturer's instructions, slides were developed with 3,3'-diaminobenzidine (DAB) (ImmPACT DAB, Vector Laboratories, CA, USA) for 5 min, washed and counterstained with hematoxylin. Light microscopy was performed on an upright microscope (Eclipse E200, Nikon, NY, USA) adapted with a Leica DFC480 camera (Leica, IL, USA).

Uniaxial tensile testing

Uniaxial tensile testing was performed in ambient air on dog-bone shaped samples with a gauge length, width and thickness of 4, 2 and 1.2 mm, respectively ($n \geq 4$). The average duration of mechanical testing from set up to completion was less than 10 s and sample dehydration was not observed. All samples were tested in uniaxial tension to failure at a strain rate of 38.4% per second using a servo electric material testing system (TestResources, MN, USA) adapted with a 25 N load cell at a sampling rate of 100 Hz. This testing protocol has been applied previously for mechanical properties testing of oligomer scaffolds [16] and rat skin [27]. Young's modulus (E_T) was calculated from the linear region of the stress strain curve. Ultimate tensile stress (UTS) represented peak stress experienced by the sample, and failure strain (ϵ_f) was the strain at which samples experienced total failure. Samples that failed outside the gauge region were excluded from data analysis.

Statistical analysis

Statistical analyses were performed using statistical analysis software (SAS, NC, USA). Unless otherwise stated, comparisons were made using one-way analysis of variance with a Tukey's *post hoc* test. A critical global p-value of 0.05 was used.

Results

Controlled confined compression of low-density oligomer matrices supports custom fabrication of dermal scaffolds

Confined compression of low-density oligomer matrices at specified strain rates has been used previously to fabricate collagen scaffolds varying in total content and spatial gradients of collagen fibrils [16,21]. Here, this method was used

to create densified dermal scaffolds, namely Oligomer-20 ($5\times$ compression of a 4 mg/cm^3 matrix to 20 mg/cm^3) and Oligomer-40 ($10\times$ compression of a 4 mg/cm^3 matrix to 40 mg/cm^3), each of which had the same final dimensions of 15.6-mm diameter and 1.2-mm thickness. Scaffold ultra and microstructures were visualized by cryo-SEM and compared with uncompressed scaffolds (Oligomer-4; 4 mg/cm^3 matrix), normal rat skin and HeliCote (commercial collagen dressing), with an emphasis on fibril density, fibril orientation and estimated scaffold pore size (Figure 2A–C).

As expected, the dermal layer of normal rat skin featured a layered construction, which was evident both qualitatively and quantitatively (Figure 2A & B) and consistent with previously published cryo-SEM studies of mammalian skin [28,29]. Fibrils and/or fibril bundles aligned in a basket-weave pattern parallel and oblique to the skin surface at all levels. The upper papillary dermis region appeared as loose, porous connective tissue bordered by dense sheets of fibrillar collagen. The underlying reticular dermis featured densely packed individual fibrils, with apparent fibril bundles aligned parallel to the surface. Estimated pore diameters for the reticular dermis ranged from 0.2 to $3\text{ }\mu\text{m}$, with more uniform and well-defined pores (on the order of $5\text{ }\mu\text{m}$) evident within the papillary dermis.

Evaluation of Oligomer-20 and Oligomer-40 revealed a greater overall collagen-fibril content compared with uncompressed Oligomer-4, with Oligomer-40 exhibiting the greatest (Figure 2). Spatial gradients differing in fibril content and orientation were apparent within Oligomer-20 and Oligomer-40 (Figure 2A & B). High-density regions near the surface appeared as aggregates or bundles of fibrils aligned parallel to the surface, with fibril density and extent of alignment decreasing with distance from the surface. Fibril alignment, which was induced during scaffold fabrication, was observed reproducibly within the upper two-thirds of Oligomer-40 scaffolds, while Oligomer-20 displayed aligned fibrils only in the upper-third region (Figure 2A & B). Toward the bottom, individual fibrils were randomly oriented, giving rise to an isotropic, porous network which was similar to that observed for uncompressed Oligomer-4. Within the porous regions, estimated pore diameters were on the order of $3\text{ }\mu\text{m}$, while more dense, aligned regions had more varied pore sizes ($0.8\text{--}3\text{ }\mu\text{m}$) similar to that of the reticular dermis. The commercial dressing, on the other hand, exhibited a dramatically different construction, with its loose, porous network formed by small meshes of fibrillar collagen microparticulate (Figure 2C). The pore size for this material was on the order of $100\text{ }\mu\text{m}$, which is consistent with published values [6] and more than an order-of-magnitude greater than that observed for rat skin and oligomer scaffolds.

Tensile properties of oligomer dermal scaffolds increase with collagen content

In addition to microstructure features, mechanical properties of fabricated collagen scaffolds are important design considerations, dictating not only macro-scale mechanical properties (e.g., handling and suturability) but also cell-collagen mechanochemical signaling. Representative stress-strain plots for oligomer scaffolds and the commercial collagen dressing are shown in Figure 3A. As expected, oligomer scaffold tensile properties increased with their overall collagen fibril content. All oligomer groups were statistically different, with E_T and UTS values ranging from $230 \pm 32.4\text{ kPa}$ and $79.7 \pm 11.81\text{ kPa}$ for Oligomer-4 to $985 \pm 265\text{ kPa}$ and $336 \pm 60.2\text{ kPa}$ for Oligomer-40 (Figures 3B & C). Mechanical properties for the commercial collagen dressing were most similar to Oligomer-20 with E_T of $753 \pm 137\text{ kPa}$ and UTS of $210 \pm 30.3\text{ kPa}$ (Figure 3B & C), despite differences in their method of fabrication and microstructure. Interestingly, no statistical difference was observed in failure strain, which measured roughly 25–30% for all materials (Figure 3D).

Oligomer-20 & oligomer-40 scaffolds persist within the wound bed & resist wound contraction

Efficacy of regenerative dermal replacements is dependent, in part, on their ability to resist wound contraction and provide a persistent biological scaffold that induces rapid cellularization, vascularization and epithelialization. To test the hypothesis that the total content and spatial gradient of collagen fibrils within oligomer scaffolds are important determinants of wound healing outcomes, scaffolds were applied to full-thickness excisional skin wounds prepared on the rat dorsum. Compressed scaffolds, which demonstrated a spatial gradient of fibrils, were placed with the porous (less dense), isotropic region near the wound base to facilitate cellular integration. Representative wound images taken on days 0, 7 and 14 for the various treatment groups are shown in Figure 4A, with normalized wound area measurements in Figure 4B. As expected, autografts were most effective at limiting wound contraction. The majority of autografts showed a cyanotic discoloration by day 7 (Figure 4A), with a small number of grafts (20%) failing to take, as evidenced by extensive necrosis and black coloration. Initial contraction of the autograft and wound site contributed to roughly a 25% decrease in wound area within the first 7 days with no further changes

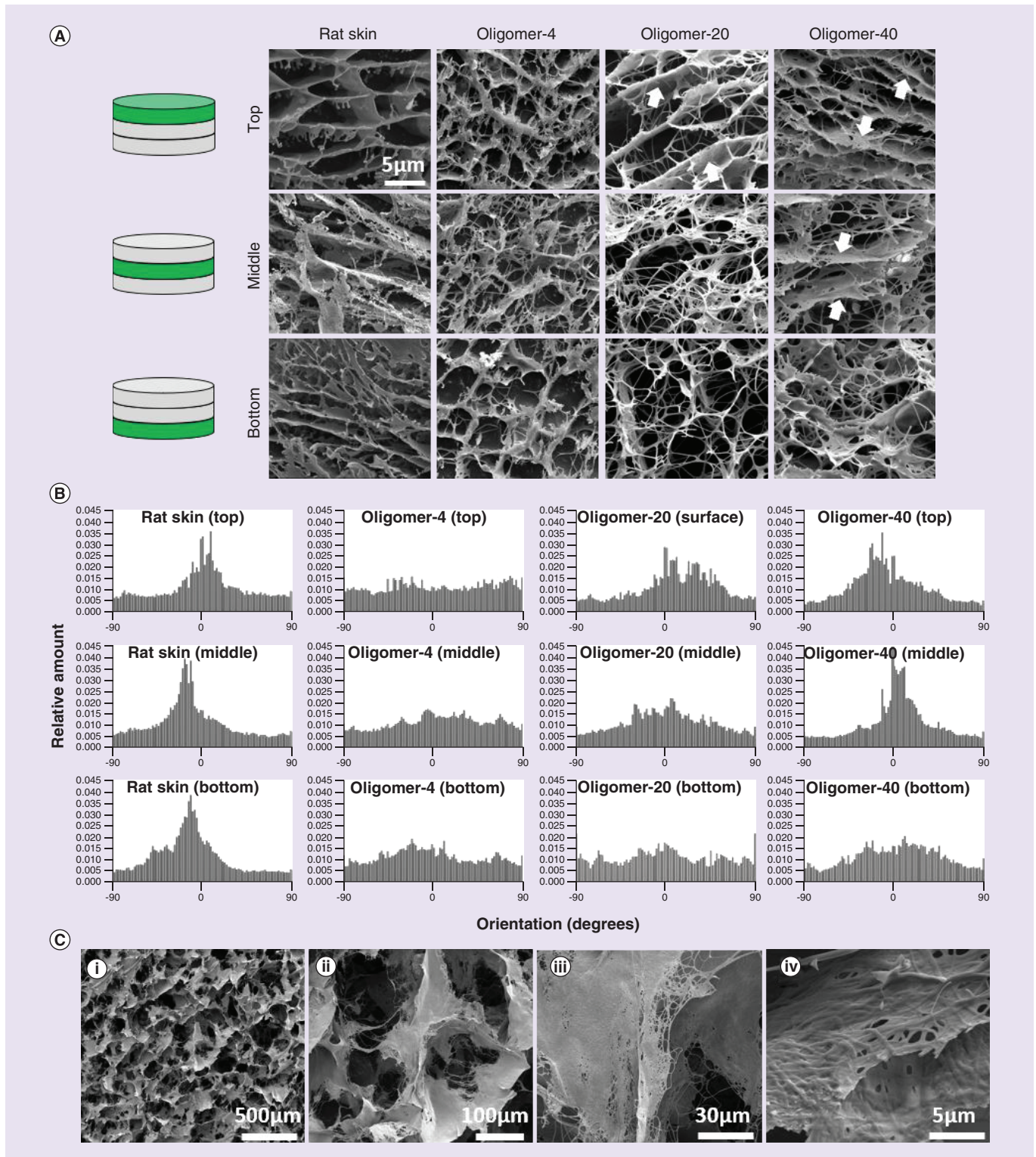


Figure 2. Microstructural analysis of oligomer dermal scaffolds, commercial collagen dressing, and rat skin. (A) Cryo-scanning electron microscopy images showing layered ultra and microstructure of normal rat skin and oligomer dermal scaffolds. Arrows highlight fibril bundling and alignment within Oligomer-20 and Oligomer-40 scaffolds. Scale bar: 5 μm . **(B)** Fibril directionality histograms for normal rat skin and oligomer dermal scaffolds. Alignment is indicated in the histogram profile, where a peak near 0 degrees corresponds to alignment parallel to the surface of the tissue. **(C)** Cryo-scanning electron microscopy images showing ultra and microstructure of commercial collagen dressing. At low magnification the relatively large porous microstructure formed by tissue microparticulate is evident (i & ii). High magnification images reveal dense fibrillar collagen within particulated tissue (iii & iv). Scale bars: (i) 500 μm ; (ii) 100 μm ; (iii) 30 μm ; (iv) 5 μm .

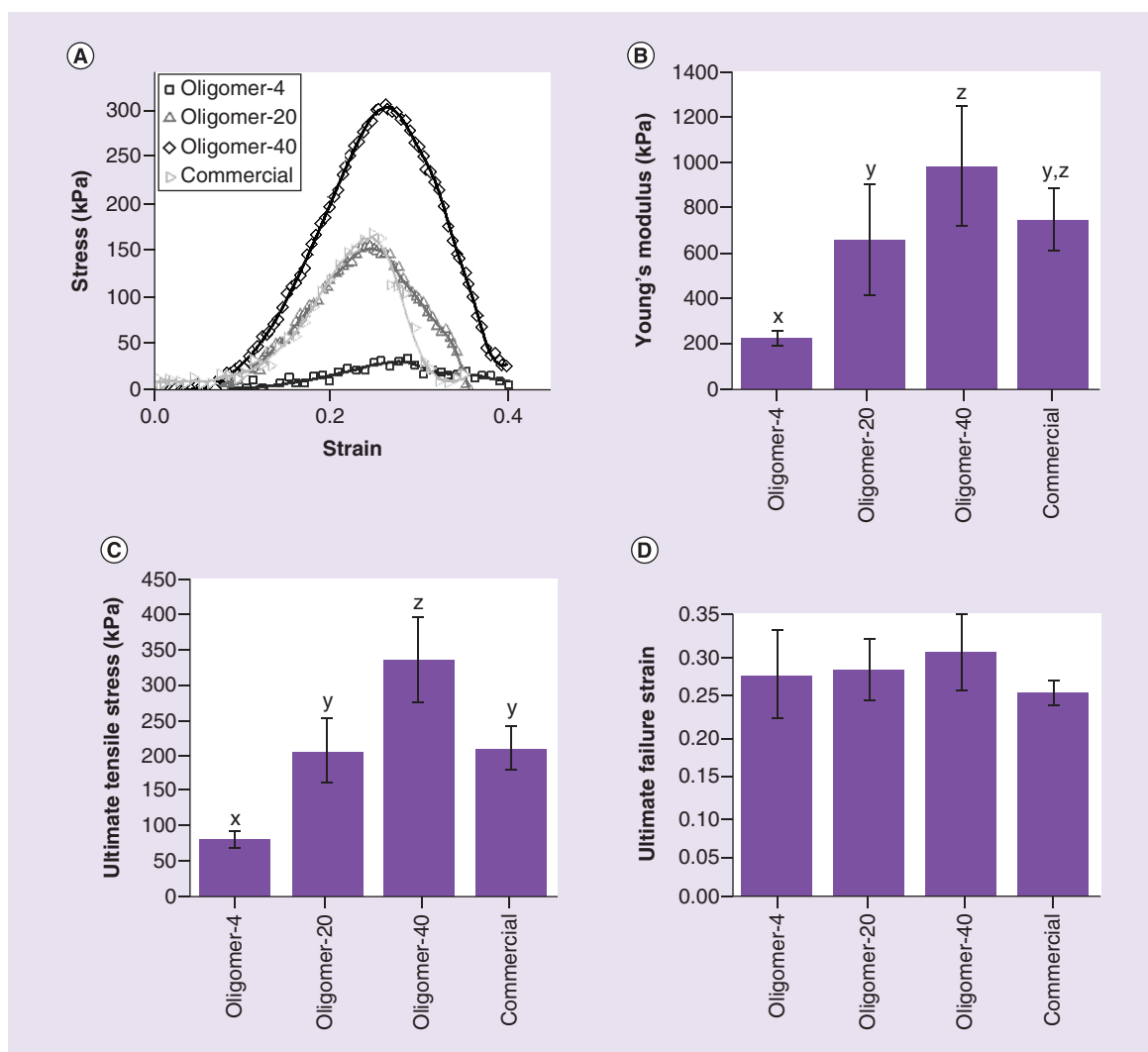


Figure 3. Tensile mechanical properties for oligomer dermal scaffolds and commercial collagen dressing. Dog-bone shaped samples with gauge length, width and thickness of 4, 2 and 1.2 mm, respectively, were subjected to uniaxial tensile loading. (A) Representative stress-strain curves, (B) Young's modulus, (C) ultimate stress and (D) failure strain, are shown (mean \pm standard deviation; $n \geq 4$). Letters indicate statistically different groups; $p < 0.05$.

observed on day 14. By contrast, unfilled wounds showed progressive and substantial contraction over the 14-day study period. At 14 days, only about 10% of the wound area remained, appearing as elongated scars with sagittal plane alignment. Similar results were observed for wounds treated with Oligomer-4 and the commercial dressing.

Interestingly, Oligomer-20 and Oligomer-40 served as dermal replacements that modulated wound contraction based on total collagen content (Figure 4A & B). Upon gross examination after 7 days, Oligomer-20 and Oligomer-40 constructs persisted within the wound bed and showed no discoloration (Figure 4A). By 14 days, these constructs showed signs of epithelialization and integration with the surrounding normal skin (Figure 4A). While Oligomer-20 and Oligomer-40 yielded statistically similar wound areas that measured roughly 50–60% at day 7, Oligomer-40 wound sizes stabilized, showing no additional significant reduction in size at day 14 (Figure 4B). By contrast, wounds treated with Oligomer-20 showed a more progressive decrease in wound size over the 14-day period; however, the observed contraction rate was decreased compared with Oligomer-4, commercial dressing, and no fill groups. Notably, both Oligomer-20 and Oligomer-40 scaffolds showed no evidence of rapid resorption or proteolytic degradation at either the 7- or 14-day time points.

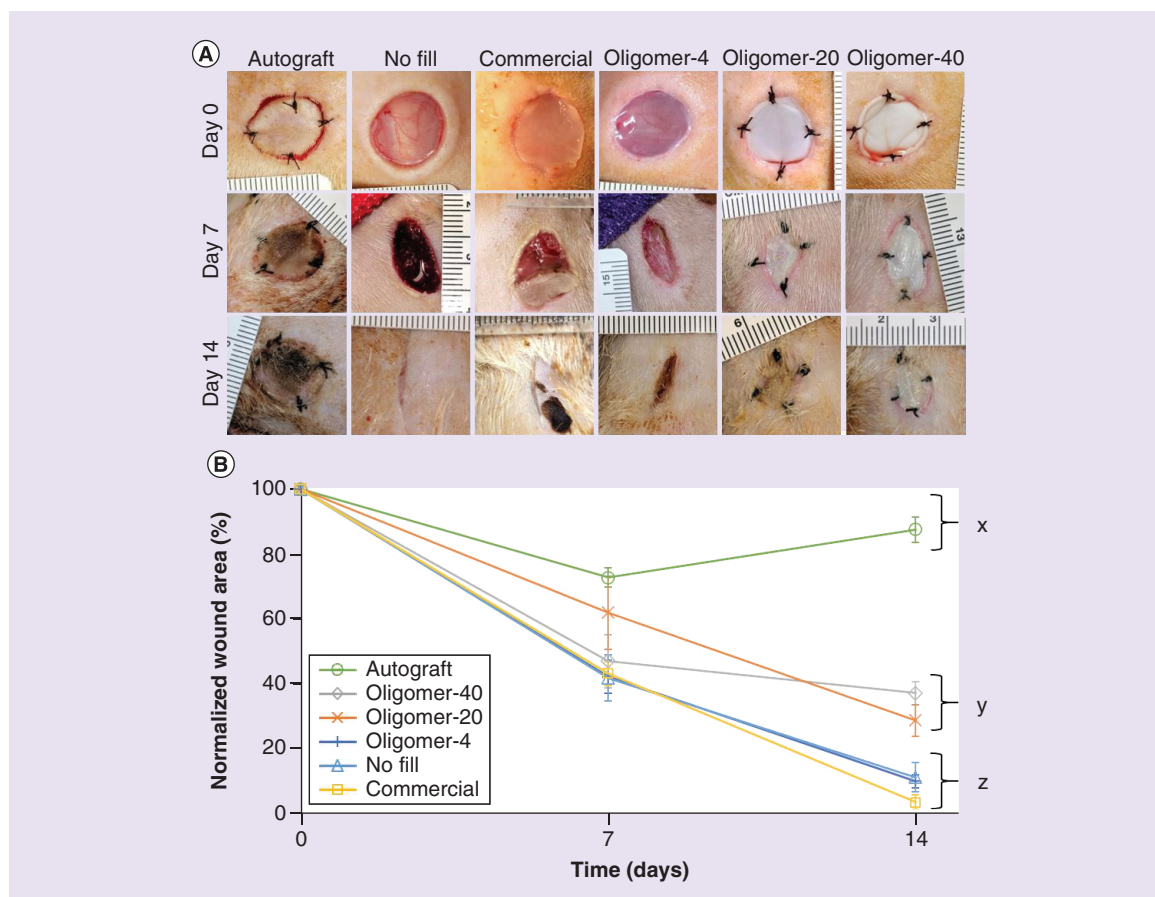


Figure 4. Time-dependent changes in wound appearance and contraction for treatment and control groups. (A) Representative gross images of full-thickness skin wounds at 0, 7 and 14 days following various treatments. **(B)** Graph showing time-dependent changes in normalized wound area for each group (mean \pm standard deviation; $n = 4-8$ for control and experimental groups). Letters indicate statistically different groups; $p < 0.05$.

Spatial gradient of collagen fibrils modulates timing & extent of cellularization & vascularization

In addition to modulating wound contraction, dermal replacements should induce rapid cellularization and vascularization to encourage tissue regeneration rather than classic wound healing with scar formation. Histopathological analysis was performed on excised tissue sections stained with hematoxylin and eosin (data not shown) as well as Masson's trichrome (Figure 5), which facilitates collagen visualization. Additionally, immunostaining for myofibroblasts (Figure 6A) and endothelial cells (Figure 6B) was used to investigate patterns of cellularization and vascularization for each treatment group.

Autograft-treated wounds showed limited revascularization and cellular infiltration over the 14-day period (Figure 5). Even in grafts which took successfully, numerous necrotic cells, including atrophying muscle cells of the panniculus carnosus muscle were evident. This tissue devitalization contributed to the development of regional inflammation, which was evident throughout the graft material, especially at 14 days. A decrease in the health and thickness of the epidermis was also noted at both 7 and 14 days. Conversely, unfilled wounds displayed the classic phases of wound healing over the 14-day period which was facilitated by substantial contraction of wound edges (Figure 5). A low-density provisional wound matrix was evident at day 7, populated by numerous inflammatory cells, including macrophages and neutrophils. By day 14, the narrowed wound area was largely populated by myofibroblasts (Figure 6A), with increased amounts of fibrillar collagen that stained dark blue, and a multilayered epithelium along the surface. By contrast, wounds treated with the commercial dressing showed limited cellular migration and vascularization at day 7 (Figure 5). By 14 days, the porous dark blue staining material showed gradual resorption, as evidenced by active proteolytic degradation and phagocytosis by macrophages and giant cells, especially within the lower regions of the material (Figure 5). As the commercial dressing degraded and the wound

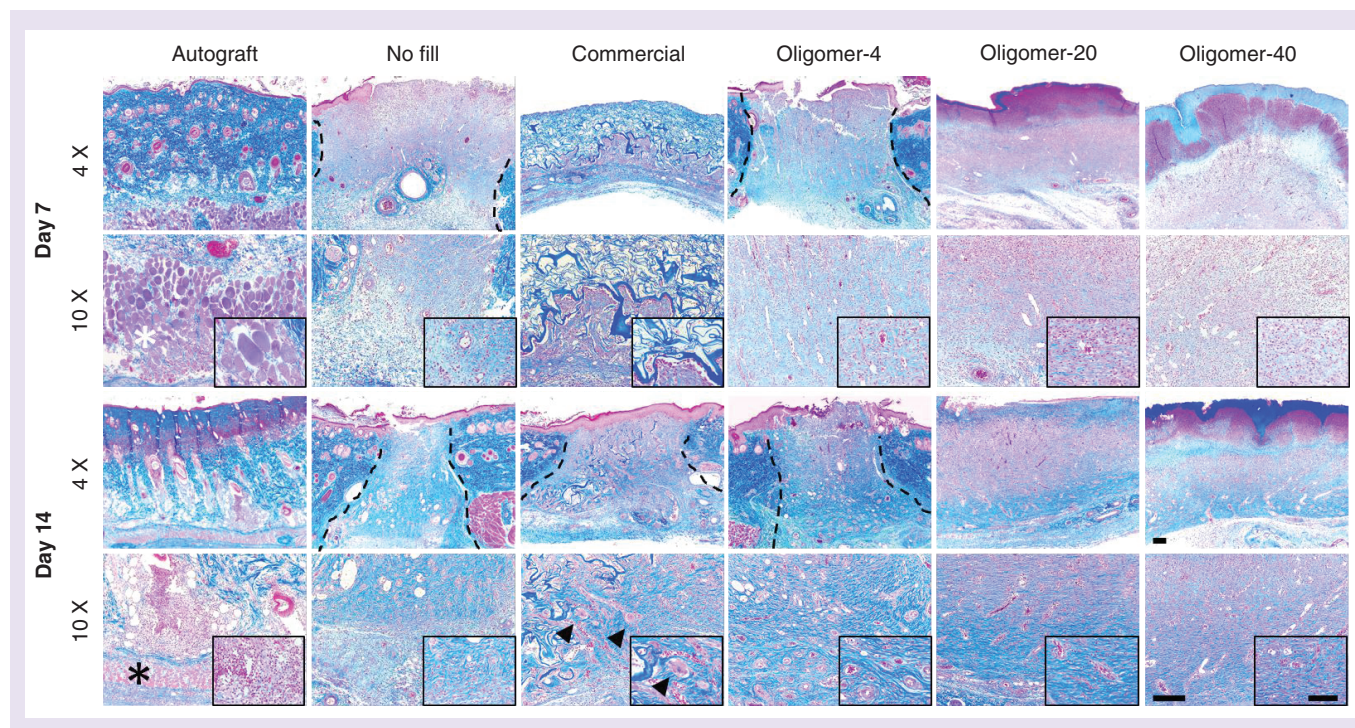


Figure 5. Histological cross-sections (4x and 10x with 40x inset) of excised skin wounds 7 days (above) and 14 days (below) stained with Masson's trichrome following treatment with autograft, no fill, commercial dressing, Oligomer-4, Oligomer-20 and Oligomer-40. Images represent center region of wound with inset focused on cellular response. Asterisks denote atrophying panniculus carnosus muscle, arrowheads denote giant cells and dashed lines indicate wound borders if visible. Scale bars: 4x: 200 μm ; 10x: 200 μm ; 40x: 100 μm .

contracted, it was replaced with fibrous collagen deposited by host cells, and neovascularization and epithelialization were evident (Figures 5 & 6B). While no myofibroblasts were observed within central regions of the commercial dressing, they were evident within areas of newly deposited collagen (Figure 6A).

All oligomer scaffolds fostered rapid cellularization and vascularization that proceeded upward and inward from the wound edges at a rate that was dependent upon fibril density and orientation (Figure 5). Although numerous mononuclear and polymorphonuclear cells infiltrated oligomer-treated wounds, limited activated macrophages and scaffold proteolysis were observed, which was especially apparent for Oligomer-20 and Oligomer-40. For these materials, light blue staining, which is a characteristic of oligomeric collagen material, persisted and was evident within the wound bed at both 7 and 14. Interestingly, the overall number of myofibroblasts observed within oligomer-treated wounds was decreased compared with the no fill controls (Figure 6A). Furthermore, the myofibroblast number decreased with increasing scaffold collagen content. Epithelialization, with identifiable stratified epidermis and stratum corneum (Figure 7), was also apparent in all oligomer-treated wounds and progressed from the wound edges toward the wound center. As expected, the extent of epithelial coverage at 14 days was increased for contracted wounds, which had a smaller area to cover.

Functional vascularization throughout Oligomer-4 was observed at 7 days, as evidenced by red blood cells within vessel lumens and CD31⁺ endothelial cells (Figures 5 & 6B). Rapid vascularization also occurred in Oligomer-20 and Oligomer-40; however, the level of penetration toward the surface was modulated by the graded microstructure (Figure 5 & 6B). More specifically, the lower two-thirds of Oligomer-20 and Oligomer-40 scaffolds were vascularized at day 7. By 14 days, this extent of vascularization progressed to near 90% for Oligomer-20 and 70% for Oligomer-40.

Discussion

Large volume and chronic nonhealing wounds continue to place a tremendous socioeconomic burden on affected individuals, clinicians, wound care specialists and payers around the world [1]. While patient autografts and

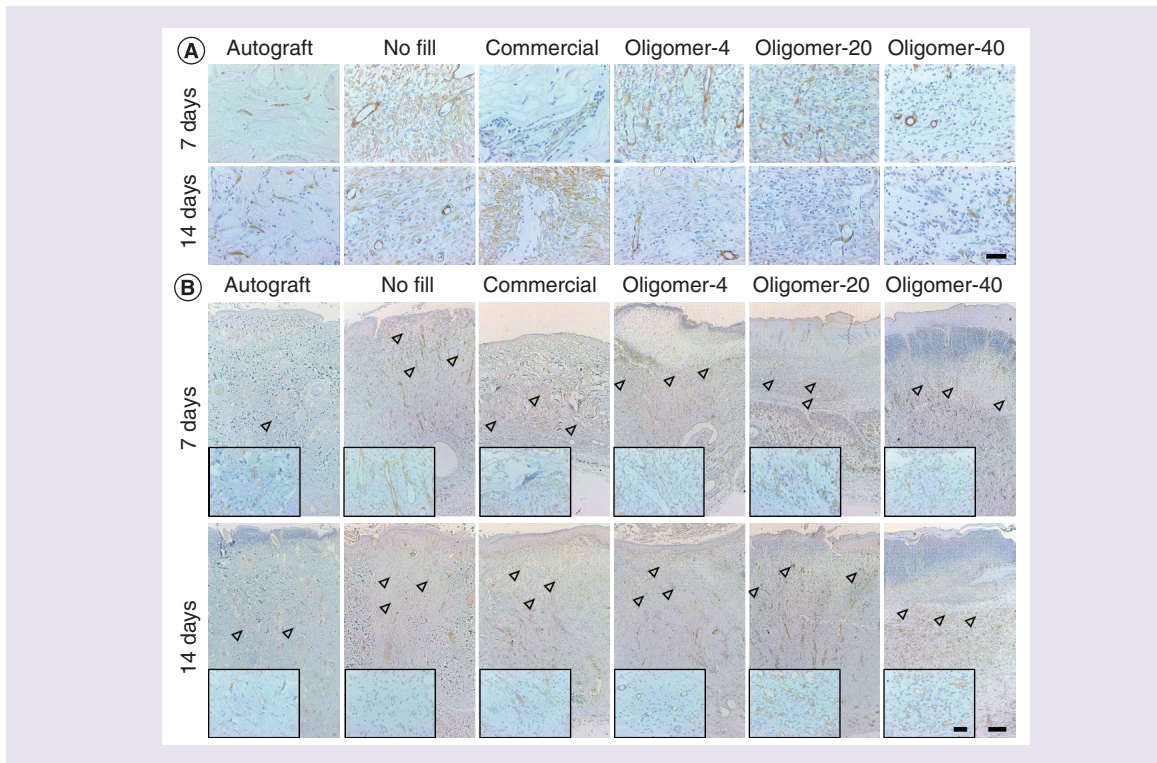


Figure 6. Time-dependent changes in cellularization and vascularization of wounds following treatment with autograft, no fill, commercial dressing, Oligomer-4, Oligomer-20 and Oligomer-40. (A) Histological cross-sections of excised wound tissues stained for blood vessel and myofibroblast marker α -SMA (brown; 7 and 14 days) and (B) endothelial cell marker CD31 (brown; 7 and 14 days). Arrowheads denote presumed level of vascularization based on presence of CD31 positive stained lumens with identifiable red blood cells. Scale bars: (A) 50 μ m; (B), inset: 50 μ m.

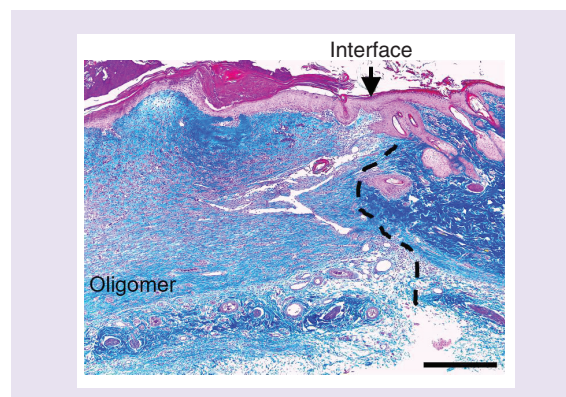


Figure 7. Histological cross-section stained with Masson's trichrome showing integration of Oligomer-20 scaffold with adjacent normal skin at 14 days. Arrowhead and dashed line indicate interface between scaffold and native tissue with epithelium migrating across wound. Scale bar: 500 μ m.

present-day dermal and dermal–epidermal substitutes remain the therapeutic strategies of choice, autografts are not always available in sufficient quantity and both autografts and skin substitutes are often associated with contracture, scarring, repeat procedures and growth limitations [30]. Dermal regeneration strategies aim to provide new therapeutic options for such wounds by restoring, as rapidly and accurately as possible, original dermal structure and function which is essential for achieving desired clinical outcomes. In this study, oligomer collagen polymers were interfaced with the scalable biomanufacturing technique confined compression for multiscale design and fabrication of fibrillar collagen scaffolds as a permanent and integrating dermal replacement. Our findings show that total collagen content, together with spatial gradients in fibril density and orientation, are important

design considerations, with these features contributing not only to scaffold-level mechanical properties but also to cellular-level mechanochemical signaling important for dermal regeneration.

Skin biomechanics and associated cell-collagen mechanobiology is fundamental to skin morphogenesis, homeostasis and repair, and has been implicated in a number of skin pathologies [11,12]. For example, conditions leading to abnormal collagen-fibril assembly and crosslinking, as observed with deficient levels of ascorbic acid (scurvy) and certain forms of Ehlers Danlos syndrome, are often associated with weak and fragile skin as well as defective wound healing [31,32]. On the other hand, extrinsically induced increases in skin tension are associated with hypertrophic scarring [33], a process that has been linked to altered cell collagen and inflammatory signaling [34]. Further corroborating evidence comes from *in vitro* studies, where fibroblasts cultured within 3D collagen matrices of varied microstructure and stiffness sense and respond to such cues by modulating their proliferation, migration, collagen deposition and contractile properties [35–38]. Likewise, endothelial cells and their progenitors respond to these cues by modulating the extent, length and morphology of vascular networks formed *in vitro* and *in vivo* [14,17,18,39]. Collectively, these results suggest that the collagen-fibril microstructure is a critical determinant of how mechanical load information is transmitted across multiple size scales, from tissue to cellular level and *vice versa*, suggesting its potential as an important design consideration for dermal regeneration therapies [11,12,40].

While collagen is recognized as a vital component to skin mechanobiology and wound healing, surprisingly few strategies have targeted the microstructure of fibrillar collagen scaffolds, largely because of challenges associated with the accurate and reproducible control of such features. Early reports of creating collagen constructs with dermal-like histology and consistency involved seeding fibroblasts within polymerized monomeric collagen matrices, and in turn, allowing the cells to contract and densify the surrounding fibrils over a 2-week period [41]. Seeding keratinocytes that formed a multilayered epidermis on the surface of this dermal equivalent gave rise to the first tissue-engineered living skin, which gained US FDA approval in 1998. In 2005, Brown reported a ‘cell-independent’ approach for densifying monomeric collagen matrices that could be applied in the presence or absence of cells [20]. Here, plastic compression in an unconfined format, along with capillary fluid flow into absorbent layers, was used to increase the collagen density by reducing the fluid content [20]. *In vitro* and *in vivo* studies by Hu [42], Ananta [43] and Braziulis [44] have applied this compression method to produce dermal or dermo-epidermal substitutes. While these approaches have contributed to the development and translation of cellularized skin equivalents, limited focus has been placed on how specific collagen microstructure features contribute to skin mechanics, mechanobiology and regeneration.

Other bioengineering approaches have targeted dermal and skin regeneration through the design and fabrication of acellular scaffolds from fibrillar collagen microparticulate, a strategy originally described by Yannas and Burke [45–47]. While this insoluble form of collagen can be swollen in dilute acid solutions, it does not exhibit the *de novo* fibril-forming capacity of monomeric and oligomeric collagens. Fabrication of these scaffolds instead involves lyophilization of viscous suspensions of bovine tendon microparticulate in the absence or presence of GAGs (chondroitin 6-sulfate) to create a freeze-dried sponge-like material. Microparticulate density, lyophilization parameters, along with various levels of exogenous glutaraldehyde and dehydrothermal crosslinking are used to control pore size, cellular adhesion and infiltration, and degradation (resorption) rate (for a recent review see [48]). This approach has yielded a portfolio of commercial collagen wound dressings, including the bilayered Integra Dermal Regeneration Template (collagen-GAG sponge covered with a thin silicone layer), which is indicated for skin replacement. Since the objective of the present study was to define the role of specific collagen scaffold microstructure features in dermal regeneration, HeliCote, a collagen sponge dressing fabricated without GAGs and exogenous crosslinking was selected for comparison.

An essential and differentiating element of our approach was the use of oligomeric collagen, an acid-soluble and fibril-forming collagen formulation that retains mature intermolecular crosslinks (e.g., histidinohydroxylysino-nor-leucine) naturally found in dermis and other connective tissues [49,50]. These crosslink chemistries are important determinants of *in vivo* collagen structure and function, serving to decrease collagen turnover rate (increase proteolytic resistance), increase fibril stability and increase tissue mechanical integrity [49,50]. Our group has also documented that these crosslinks are critical to the *in vitro* fibril-forming properties of purified oligomeric collagen, giving rise to fibrillar collagen scaffolds that better approximate those within the body’s tissues [51]. Type I oligomeric collagen exhibits not only fibrillar but also suprafibrillar assembly, yielding highly interconnected collagen-fibril scaffolds with substantially improved proteolytic resistance and mechanical integrity compared with conventional monomeric collagens (atelocollagen and telocollagen) [13,15]. Collectively, this connectivity exhibited at both the

molecular and fibrillar size scales defines the multiscale structure and mechanical properties of polymerized oligomer scaffolds [15,16].

As unmodified natural collagen polymers, oligomers are well suited for tissue engineering and regenerative medicine applications, since the collagen primary sequence and associated crosslink chemistries are highly conserved between species [50,52]. For this study, oligomeric collagen was derived from porcine dermis, since this tissue source is readily available and can be obtained from specific pathogen free herds, facilitating translation into the clinic. Although concerns have been raised in the past regarding immunogenicity of xenogeneic collagen, contributions of material format, processing and impurities (e.g., cellular by-products and denatured collagen) have yet to be fully delineated [53]. To date, no evidence of pathological immunogenicity has been observed with oligomer materials when implanted in different species and tissue microenvironments, which is likely due to their high-level purity as well as the absence of exogenous additives and crosslinking [14,18,54–58]. In this way, the multi-faceted biosignaling capacity inherent to collagen fibrils is preserved, including integrin-mediated cell adhesion [59], ECM molecule and soluble factor (e.g., growth factors) binding and sequestration [59] and immune modulation [60,61].

For this work, plastic compression was applied to low-density oligomer matrices in a confined (rather than an unconfined) format to controllably modulate the collagen-fibril microstructure. Interestingly, this approach is not suitable for monomeric collagen matrices due to the inability of their fibril microstructure to sustain or support associated compressive and fluid shear forces [16]. It is noteworthy that confined compression provides control over both the amount and direction of fluid removal, facilitating customization of spatial gradients in fibril density and orientation. Specifically, total collagen content of the compressed scaffold is controlled through modulation of the starting volume and concentration of the original scaffold together with the applied compressive strain [16,21]. Additionally, strain rate can be varied to control steepness of the fibril density gradient, and placement of porous polyethylene foam and associated porous-solid boundary condition can be used to define high-order spatial fibril organization (e.g., alignment and directional gradient) (see [19] for a more detailed review).

All oligomer scaffolds fabricated for this study featured a randomly oriented, porous fibrillar network near the bottom. Oligomer-20 and Oligomer-40 were fashioned with a vertical gradient in fibril density, with varied extents of fibril alignment and bundling near their surface to recapitulate some of the anisotropies found in normal dermis. In terms of estimated pore sizes, oligomer scaffolds were most similar to that of normal rat dermis and more than an order of magnitude less than HeliCote. Although, the pore size for bioengineered collagen sponge dressings has been rigorously documented as a critical design feature for controlling cellularization and vascularization [48], there is no reason to *a priori* believe the optimal porosity for collagen sponges and oligomer scaffolds would be the same. While both HeliCote and oligomer scaffolds are primarily composed of fibrillar collagen and noncrosslinked, their fundamental design and method of fabrication is different, ultimately yielding scaffolds with different overall microstructures, mechanical properties and mechanisms of action. Further to this point, while the bulk tensile properties for HeliCote were statistically similar to Oligomer-20, the *in vivo* tissue responses of these two materials were dramatically different. In summary, the Young's modulus for oligomer scaffolds ranged from 0.2 MPa for Oligomer-4 to nearly 1 MPa for Oligomer-40, which falls within reported ranges for human cornea (0.1–11.1 MPa), aorta (0.6–3.5 MPa) and dermis (0.6–15 MPa) [62,63]. The bulk mechanical properties of Oligomer-20 and Oligomer-40, but not Oligomer-4, facilitated handling and suturing in place.

When evaluated within an established full-thickness excisional skin model, the dense microstructure of autograft skin was most effective at minimizing contraction but showed delayed cellularization and vascularization. In the present study, roughly 20% of autografts were unable to re-establish the necessary nutrient flow prior to necrosis and failed to take. This observed graft failure rate is consistent with previously reported values for rodent models [64]. Additionally, as expected, no fill controls healed primarily by contraction over the 14-day period. The tissue response observed with the commercial dressing was also consistent with its design [65], with controlled infiltration of cells and progressive active scaffold degradation occurring via inflammatory mediators, most notably macrophages and giant cells, over the 2-week period. This observed high rate of degradation (resorption) and wound contraction are consistent with other published studies in rodents [66] and can be attributed to the absence of GAGs and exogenous crosslinking, which are known to slow these processes [48].

The provision of densified oligomer dermal scaffolds that persisted within the wound bed and integrated with surrounding normal tissue, was effective at limiting both wound contraction and the myofibroblast phenotype. Oligomer-20 and Oligomer-40 scaffolds appeared to recapitulate, in part, the stress-shielding provided by normal dermal collagen, where fibroblasts adopt their spindle-shaped morphology and downregulate α -SMA [5]. In this case, the relatively rigid fibrillar microstructure provided by these scaffolds was sufficient to resist significant

cellular contraction, while supporting the necessary cellular traction forces to facilitate migration. Recent work has shown that fibroblast phenotype and behavior, including apoptosis signaling, matrix metalloproteinase activity and differentiation into myofibroblasts, are strongly linked to the rigidity or laxity of the ECM, even independent of TGF- β signaling [67,68]. By persisting and modulating fibroblast function, these oligomer scaffolds appear to circumvent contraction and reduce the burden on host cells to deposit collagen and rebuild the dermis, which collectively speeds up the healing process and improves outcomes. To the best of our knowledge this is the first report of self-assembled collagen materials that persist and integrate, effectively decreasing cutaneous wound contraction and the myofibroblast phenotype in absence of exogenous crosslinking or reinforcing materials.

There has been significant interest in designing dermal and skin replacements with improved vascularization, with the majority of approaches involving soluble angiogenic factors, such as FGF2 and VEGF, either alone or in combination with other matrix molecules [69,70]. Here, we show that Oligomer-20 and Oligomer-40 were not only effective inhibitors of contraction but also promoters of vascularization, which is critical to dermal regeneration as well as the support of epithelialization or a secondarily applied epidermal layer. Vessel networks were well-formed at 2 weeks, staining for both CD31 and α -SMA. However, an interesting finding was that the fibril bundling and alignment within scaffolds appeared to hinder or delay vessel progression toward the surface. Such findings are consistent with observations for decellularized tissue scaffolds, which are reported to require 2–4 weeks to vascularize sufficiently to support overlying split-thickness skin grafts, and the fact that human auto or allografts thicker than 0.4 mm show delayed angiogenesis and failure to take [71,72].

Conclusion

This work serves as an important first step in development of mechano-instructive dermal scaffolds that promote rapid cellularization and vascularization while simultaneously reducing wound contraction and scarring. We show custom fabrication of dermal replacements with high bulk mechanical integrity that facilitate handling and suturing, factors that are important for adoption by wound care specialists and surgeons. Our work also documents that oligomer scaffolds persist, restoring important mechanobiological cues by serving as a surrogate dermis. Finally, our findings show that precision tuning collagen-fibril microstructure can be used to modulate mechanotransduction pathways involved in tissue regeneration. This study has some limitations. While no animal model perfectly replicates wound healing in humans, important information can be inferred from established animal models, such as the rodent full-excisional skin model used here. Follow-up experimental and computational modeling studies are now underway to further define how specific microstructural features of oligomer scaffolds affect, more broadly, multiscale mechanical properties as well as mechanotransduction mechanisms underlying cellularization, vascularization and epithelialization. Finally, studies involving large animal wound models as well as models of compromised healing are necessary to further validate efficacy and scalability of our approach.

Translational perspective

Tissue-engineered dermal replacements have now become a well-established part of clinical care for difficult-to-treat wounds. This study represents an advancement in the bio-inspired design of dermal replacements that can reduce morbidity and mortality of patients with severe and difficult-to-heal wounds by regenerating lost tissue while preventing scar formation. Our design strategy involves creation of persistent fibrillar collagen scaffolds whose microstructure is defined and designed to promote skin regeneration by re-establishing mechanical continuity across the tissue and cellular size scales, restoring essential skin mechanobiology. Oligomeric collagen was manufactured and standardized from porcine dermis according to relevant ASTM International standards for polymerizable (fibril-forming) collagens. Oligomer scaffold microstructures were customized using confined plastic compression, a scalable and controllable biomanufacturing process. This initial preclinical study documented that total content and spatial gradients in collagen-fibril density and orientation are important considerations when designing scaffolds to promote rapid cellularization and vascularization while simultaneously preventing wound contraction. Further mechanistic-based design iterations along with preclinical evaluation in large animal wound models is needed to further validate the translational potential of our strategy.

Author contributions

DO Sohuts kay, KP Buno and SL Voytik-Harbin conceived and designed research, analyzed data, and interpreted results. DO Sohuts kay, KP Buno and SJ Nier performed experiments with input and guidance from SS Tholpady. DO Sohuts kay, KP Buno and SL

Voytik-Harbin prepared figures and drafted the manuscript. All authors reviewed the manuscript and SL Voytik-Harbin approved final version of manuscript.

Acknowledgments

The authors acknowledge the assistance of V Bernal-Crespo and the Purdue University Histology Research Laboratory (a core facility of the NIH-funded Indiana Clinical and Translational Science Institute), the assistance of R Seiler and the Purdue Life Science Microscopy Facility for cryo-SEM, the assistance of A Aboelzahab for facilitating 3D-printing and provision of laboratory resources and the assistance of M Bible and T Cleary for veterinary technician and surgical experiment assistance.

Financial & competing interests disclosure

This work was funded in part by the NIH T32 Bioengineering Interdisciplinary Training for Diabetes Research Program Fellowship (NIDDK T32-DK-101000; DO Sohutskey) and NSF Graduate Research Fellowship (DGE-1333468; KP Buno). Voytik-Harbin has significant financial interest in GeniPhys, LLC, a small business that she founded to assist with the commercialization of tissue engineering and regenerative medicine technologies such as those described here. Type I oligomeric collagen and associated custom fabricated materials are the subject matter of issued and pending patents that are owned by Purdue Research Foundation and licensed to GeniPhys, LLC. The authors have no other relevant affiliations or financial involvement with any organization or entity with a financial interest in or financial conflict with the subject matter or materials discussed in the manuscript apart from those disclosed.

No writing assistance was utilized in the production of this manuscript.

Ethical conduct of research

The authors state that they have obtained appropriate institutional review board approval or have followed the principles outlined in the Declaration of Helsinki for all human or animal experimental investigations. In addition, for investigations involving human subjects, informed consent has been obtained from the participants involved.

Summary points

- Difficult-to-heal wounds are a significant burden on patients, providers and the healthcare system as a whole.
- Current wound management strategies include conservative treatment, skin grafting and tissue engineered replacements; however, scarring and loss-of-function continue to be common outcomes for patients with severe wounds.
- Our dermal regeneration strategy targets fabrication of fibrillar collagen scaffolds, whose microstructure is defined and controlled to restore necessary mechanochemical signaling by supporting the reciprocal transmission of mechanical forces across tissue and cellular size scales.
- Oligomeric collagen, a fibril-forming collagen that retains intermolecular crosslinks and exhibits improved persistence and mechanical stability, together with confined plastic compression was used to create scaffolds with varied total content and spatial gradients of collagen fibrils.
- We evaluated three groups, Oligomer-4, Oligomer-20 and Oligomer-40 against a commercial absorbable collagen sponge, no fill control and autograft skin within a rat full-thickness excisional skin model.
- The dense collagen fibril microstructure of autograft skin was most effective at decreasing wound contraction but hindered vascularization leading to tissue necrosis and 20% graft loss.
- No fill wounds displayed a classic healing response with rapid contraction.
- A commercial noncrosslinked collagen sponge fabricated by lyophilization of fibrillar collagen microparticulate, rapidly resorbed over the 14-day period via inflammatory mediated degradation and did not inhibit wound contraction.
- The rate and extent of contraction decreased as the total collagen content of oligomer scaffolds increased.
- A vertical gradient in fibril density and orientation that proceeded from a porous, isotropic organization to a high density of bundled fibrils oriented parallel to the surface facilitated rapid cellularization, vascularization and epithelialization.
- Oligomer scaffolds did not rapidly degrade but rather persisted within the wound bed where they modulated cellular traction and contraction forces based on their microstructure features.
- Additional investigations are necessary to further the mechanistic-based design and fabrication of oligomer scaffolds to promote skin regeneration for treatment of difficult-to-heal wounds.

References

1. Sen CK, Gordillo GM, Roy S *et al.* Human skin wounds: a major and snowballing threat to public health and the economy. *Wound Repair Regen.* 17(6), 763–771 (2009).

2. Harrison CA, Macneil S. The mechanism of skin graft contraction: an update on current research and potential future therapies. *Burns* 34(2), 153–163 (2008).
3. Donegan RJ, Schmidt BM, Blume PA. An overview of factors maximizing successful split-thickness skin grafting in diabetic wounds. *Diabetic Foot Ankle* 5(1), 24769 (2014).
4. Macneil S. Biomaterials for tissue engineering of skin. *Mater. Today* 11(5), 26–35 (2008).
5. Tomasek JJ, Gabbiani G, Hinz B, Chaponnier C, Brown RA. Myofibroblasts and mechano-regulation of connective tissue remodelling. *Nat. Rev. Mol. Cell Biol.* 3(5), 349–363 (2002).
6. Yannas IV, Tzeranis DS, So PTC. Regeneration of injured skin and peripheral nerves requires control of wound contraction, not scar formation. *Wound Repair Regen.* 25(2), 177–191 (2017).
7. Eming SA, Martin P, Tomic-Canic M. Wound repair and regeneration: mechanisms, signaling, and translation. *Sci. Transl. Med.* 6(265), 265sr266 (2014).
8. Young PK, Grinnell F. Metalloproteinase activation cascade after burn injury: a longitudinal analysis of the human wound environment. *J. Invest. Dermatol.* 103(5), 660–664 (1994).
9. Wiegand C, Schönfelder U, Abel M, Ruth P, Kaatz M, Hipler U-C. Protease and pro-inflammatory cytokine concentrations are elevated in chronic compared to acute wounds and can be modulated by collagen type I *in vitro*. *Arch. Dermatol. Res.* 302(6), 419–428 (2010).
10. Rennert RC, Rodrigues M, Wong VW *et al*. Biological therapies for the treatment of cutaneous wounds: Phase III and launched therapies. *Expert Opin. Biol. Ther.* 13(11), 1523–1541 (2013).
11. Wong VW, Akaishi S, Longaker MT, Gurtner GC. Pushing back: wound mechanotransduction in repair and regeneration. *J. Invest. Dermatol.* 131(11), 2186–2196 (2011).
12. Agha R, Ogawa R, Pietramaggiori G, Orgill DP. A review of the role of mechanical forces in cutaneous wound healing. *J. Surg. Res.* 171(2), 700–708 (2011).
13. Kregar ST, Bell BJ, Bailey J *et al*. Polymerization and matrix physical properties as important design considerations for soluble collagen formulations. *Biopolymers* 93(8), 690–707 (2010).
14. Bailey JL, Critser PJ, Whittington C, Kuske JL, Yoder MC, Voytik-Harbin SL. Collagen oligomers modulate physical and biological properties of three-dimensional self-assembled matrices. *Biopolymers* 95(2), 77–93 (2011).
15. Whittington CF, Brandner E, Teo KY, Han B, Nauman E, Voytik-Harbin SL. Oligomers modulate interfibril branching and mass transport properties of collagen matrices. *Microsc. Microanal.* 19(5), 1323–1333 (2013).
16. Blum KM, Novak T, Watkins L *et al*. Acellular and cellular high-density, collagen-fibril constructs with suprafibrillar organization. *Biomater. Sci.* 4(4), 711–723 (2016).
17. Whittington CF, Yoder MC, Voytik-Harbin SL. Collagen-polymer guidance of vessel network formation and stabilization by endothelial colony forming cells *in vitro*. *Macromol. Biosci.* 13(9), 1135–1149 (2013).
18. Critser PJ, Kregar ST, Voytik-Harbin SL, Yoder MC. Collagen matrix physical properties modulate endothelial colony forming cell-derived vessels *in vivo*. *Microvasc. Res.* 80(1), 23–30 (2010).
19. Sohuts kay DO, Puls TJ, Voytik-Harbin SL. Collagen self-assembly: biophysics and biosignaling for advanced tissue generation. In: *Multi-scale Extracellular Matrix Mechanics and Mechanobiology* Zhang KY (Ed.). Springer International Publishing, Cham, Switzerland, 203–245 (2020).
20. Brown RA, Wiseman M, Chuo CB, Cheema U, Nazhat SN. Ultrarapid engineering of biomimetic materials and tissues: fabrication of nano- and microstructures by plastic compression. *Adv. Funct. Mater.* 15(11), 1762–1770 (2005).
21. Novak T, Seelbinder B, Twitchell CM, Van Donkelaar CC, Voytik-Harbin SL, Neu CP. Mechanisms and microenvironment investigation of cellularized high density gradient collagen matrices via densification. *Adv. Funct. Mater.* 26(16), 2617–2628 (2016).
22. Wang J, Wang L, Zhou Z *et al*. Biodegradable polymer membranes applied in guided bone/tissue regeneration: a review. *Polymers* 8(4), 115 (2016).
23. ASTM International. ASTM F3089-14, Standard Guide for Characterization and Standardization of Polymerizable Collagen-Based Products and Associated Collagen–Cell Interactions. (2014). www.astm.org/Standards/F3089.htm.
24. Takeuchi H, Ishida M, Furuya A, Todo H, Urano H, Sugibayashi K. Influence of skin thickness on the *in vitro* permeabilities of drugs through Sprague-Dawley rat or yucatan micropig skin. *Biol. Pharm. Bull.* 35(2), 192–202 (2012).
25. Hotaling NA, Bharti K, Kriel H, Simon Jr CG. DiameterJ: a validated open source nanofiber diameter measurement tool. *Biomaterials* 61, 327–338 (2015).
26. Anguiano M, Castilla C, Maška M *et al*. Characterization of three-dimensional cancer cell migration in mixed collagen-Matrigel scaffolds using microfluidics and image analysis. *PLoS ONE* 12(2), e0171417 (2017).
27. Dombi GW, Haut RC, Sullivan WG. Correlation of high-speed tensile strength with collagen content in control and lathyrus rat skin. *J. Surg. Res.* 54(1), 21–28 (1993).
28. Tan G, Xu P, Lawson LB *et al*. Hydration effects on skin microstructure as probed by high-resolution cryo-scanning electron microscopy and mechanistic implications to enhanced transcutaneous delivery of biomacromolecules. *J. Pharm. Sci.* 99(2), 730–740 (2010).

29. Meyer W, Kacza J, Zschemisch N-H, Godynicki S, Seeger J. Observations on the actual structural conditions in the stratum superficiale dermidis of porcine ear skin, with special reference to its use as model for human skin. *Ann. Anat.* 189(2), 143–156 (2007).
30. Bottcher-Haberzeth S, Biedermann T, Reichmann E. Tissue engineering of skin. *Burns* 36(4), 450–460 (2010).
31. Myllyharju J, Kivirikko KI. Collagens and collagen-related diseases. *Ann. Med.* 33(1), 7–21 (2001).
32. Prockop DJ, Kivirikko KI. Collagens: molecular biology, diseases, and potentials for therapy. *Annu. Rev. Biochem.* 64(1), 403–434 (1995).
33. Aarabi S, Bhatt KA, Shi Y *et al.* Mechanical load initiates hypertrophic scar formation through decreased cellular apoptosis. *FASEB J.* 21(12), 3250–3261 (2007).
34. Wong VW, Rustad KC, Akaishi S *et al.* Focal adhesion kinase links mechanical force to skin fibrosis via inflammatory signaling. *Nat. Med.* 18(1), 148–152 (2011).
35. Hadjipanayi E, Mudera V, Brown RA. Close dependence of fibroblast proliferation on collagen scaffold matrix stiffness. *J. Tissue Eng. Regen. Med.* 3(2), 77–84 (2009).
36. Hadjipanayi E, Mudera V, Brown RA. Guiding cell migration in 3D: a collagen matrix with graded directional stiffness. *Cell Motil. Cytoskeleton* 66(3), 121–128 (2009).
37. Pizzo AM, Kokini K, Vaughn LC, Waisner BZ, Voytik-Harbin SL. Extracellular matrix (ECM) microstructural composition regulates local cell-ECM biomechanics and fundamental fibroblast behavior: a multidimensional perspective. *J. Appl. Physiol.* 98(5), 1909–1921 (2005).
38. Grinnell F, Petroll WM. Cell motility and mechanics in three-dimensional collagen matrices. *Annu. Rev. Cell Dev. Biol.* 26, 335–361 (2010).
39. Buno KP, Chen X, Weibel JA *et al.* *In vitro* multitissue interface model supports rapid vasculogenesis and mechanistic study of vascularization across tissue compartments. *ACS Appl. Mater. Interfaces* 8(34), 21848–21860 (2016).
40. Roeder BA, Kokini K, Voytik-Harbin SL. Fibril microstructure affects strain transmission within collagen extracellular matrices. *J. Biomech. Eng.* 131(3), 031004 (2009).
41. Bell E, Sher S, Hull B *et al.* The reconstitution of living skin. *J. Invest. Dermatol.* 81(Suppl. 1), 2S–10S (1983).
42. Hu K, Shi H, Zhu J *et al.* Compressed collagen gel as the scaffold for skin engineering. *Biomed. Microdevices* 12(4), 627–635 (2010).
43. Ananta M, Brown RA, Mudera V. A rapid fabricated living dermal equivalent for skin tissue engineering: an *in vivo* evaluation in an acute wound model. *Tissue Eng. Part A* 18(3–4), 353–361 (2012).
44. Braziulis E, Diez M, Biedermann T *et al.* Modified plastic compression of collagen hydrogels provides an ideal matrix for clinically applicable skin substitutes. *Tissue Eng. Part C Meth.* 18(6), 464–474 (2012).
45. Yannas IV, Burke JF. Design of an artificial skin. I. Basic design principles. *J. Biomed. Mater. Res.* 14(1), 65–81 (1980).
46. Yannas IV, Burke JF, Gordon PL, Huang C, Rubenstein RH. Design of an artificial skin. II. Control of chemical composition. *J. Biomed. Mater. Res.* 14(2), 107–132 (1980).
47. Dagalakis N, Flink J, Stasikelis P, Burke JF, Yannas IV. Design of an artificial skin. Part III. Control of pore structure. *J. Biomed. Mater. Res.* 14(4), 511–528 (1980).
48. Yannas IV, Tzeranis D, So PT. Surface biology of collagen scaffold explains blocking of wound contraction and regeneration of skin and peripheral nerves. *Biomed. Mater.* 11(1), 014106 (2015).
49. Eyre DR, Paz MA, Gallop PM. Cross-linking in collagen and elastin. *Annu. Rev. Biochem.* 53, 717–748 (1984).
50. Eyre DR, Wu J-J. Collagen Cross-Links. In: *Collagen: Primer in Structure, Processing and Assembly* Brinckmann J, Notbohm H, Müller PK (Eds). Springer Berlin Heidelberg, Berlin, Heidelberg, 207–229 (2005).
51. Verzijl N, Degroot J, Thorpe SR *et al.* Effect of collagen turnover on the accumulation of advanced glycation end products. *J. Biol. Chem.* 275(50), 39027–39031 (2000).
52. Stover DA, Verrelli BC. Comparative vertebrate evolutionary analyses of Type I collagen: potential of *COL1a1* gene structure and intron variation for common bone-related diseases. *Mol. Biol. Evol.* 28(1), 533–542 (2010).
53. Lynn A, Yannas I, Bonfield W. Antigenicity and immunogenicity of collagen. *J. Biomed. Mater. Res., B. Appl. Biomater.* 71(2), 343–354 (2004).
54. Stephens CH, Orr KS, Acton AJ *et al.* *In situ* type I oligomeric collagen macroencapsulation promotes islet longevity and function *in vitro* and *in vivo*. *Am. J. Physiol. Endocrinol. Metab.* 315(4), E650–E661 (2018).
55. Brookes S, Voytik-Harbin S, Zhang H, Zhang L, Halum S. Motor endplate-expressing cartilage-muscle implants for reconstruction of a denervated hemilarynx. *Laryngoscope* 129(6), 1293–1300 (2018).
56. Brookes S, Voytik-Harbin S, Zhang H, Halum S. Three-dimensional tissue-engineered skeletal muscle for laryngeal reconstruction. *Laryngoscope* 128(3), 603–609 (2018).
57. Zhang H, Voytik-Harbin S, Brookes S *et al.* Use of autologous adipose-derived mesenchymal stem cells for creation of laryngeal cartilage. *Laryngoscope* 128(4), E123–E129 (2018).

58. Critser PJ, Voytik-Harbin SL, Yoder MC. Isolating and defining cells to engineer human blood vessels. *Cell Prolif.* 44(Suppl. 1), 15–21 (2011).
59. An B, Lin Y-S, Brodsky B. Collagen interactions: drug design and delivery. *Adv. Drug Del. Rev.* 97, 69–84 (2016).
60. Kuczek DE, Larsen AMH, Thorseth ML *et al.* Collagen density regulates the activity of tumor-infiltrating T cells. *J. Immunother. Cancer* 7(1), 68 (2019).
61. Lebbink RJ, De Ruiter T, Adelmeyer J *et al.* Collagens are functional, high affinity ligands for the inhibitory immune receptor LAIR-1. *J. Exp. Med.* 203(6), 1419–1425 (2006).
62. Mckee CT, Last JA, Russell P, Murphy CJ. Indentation versus tensile measurements of Young's modulus for soft biological tissues. *Tissue Eng. Part B Rev.* 17(3), 155–164 (2011).
63. Silver FH, Seehra GP, Freeman JW, Devore D. Viscoelastic properties of young and old human dermis: a proposed molecular mechanism for elastic energy storage in collagen and elastin. *J. Appl. Polym. Sci.* 86(8), 1978–1985 (2002).
64. Pakyari M, Farokhi A, Khosravi-Maharlooie M, Kilani RT, Ghahary A, Brown E. A new method for skin grafting in murine model. *Wound Repair Regen.* 24(4), 695–704 (2016).
65. Mahesh L, Kurtzman GM, Shukla S. Regeneration in periodontics: collagen—a review of its properties and applications in dentistry. *Compend. Contin. Educ. Dent.* 36(5), 358–363 (2015).
66. Shafritz TA, Rosenberg LC, Yannas IV. Specific effects of glycosaminoglycans in an analog of extracellular matrix that delays wound contraction and induces regeneration. *Wound Repair Regen.* 2(4), 270–276 (1994).
67. Hinz B. The myofibroblast: paradigm for a mechanically active cell. *J. Biomech.* 43(1), 146–155 (2010).
68. Tracy LE, Minasian RA, Catterson EJ. Extracellular matrix and dermal fibroblast function in the healing wound. *Adv. Wound Care* 5(3), 119–136 (2016).
69. Nillesen S, Lammers G, Wismans R *et al.* Design and *in vivo* evaluation of a molecularly defined acellular skin construct: reduction of early contraction and increase in early blood vessel formation. *Acta Biomater.* 7(3), 1063–1071 (2011).
70. Shilo S, Roth S, Amzel T *et al.* Cutaneous wound healing after treatment with plant-derived human recombinant collagen flowable gel. *Tissue Eng. Part A* 19(13-14), 1519–1526 (2013).
71. Sahota PS, Burn JL, Heaton M *et al.* Development of a reconstructed human skin model for angiogenesis. *Wound Repair Regen.* 11(4), 275–284 (2003).
72. Macneil S. Progress and opportunities for tissue-engineered skin. *Nature* 445(7130), 874–880 (2007).